JOURNAL OF Materials CHEMISTRY

Two spin-containing fragments connected by a two-electron one-center heteroatom π spacer. A new open-shell organic molecule with a singlet ground state

Ll. Viadel,[a] J. Carilla,[a] E. Brillas,[b] A. Labarta[c] and L. Juliá*[a]

[a] *Departament de Química Orgànica Biològica, Centre d'Investigació i Desenvolupament (CISC), Jordi Girona 18–26, 08034 Barcelona, Spain*

[b] *Departament de Química Física, Universitat de Barcelona, Avgda. Diagonal 647, 08028 Barcelona, Spain*

[c] *Departament de Física Fonamental, Universitat de Barcelona, Avgda. Diagonal 647, 08028 Barcelona, Spain*

The synthesis of 4,4-iminobis(2,2′,2″,4′,4″,6,6′,6″-octachlorotriphenylmethyl) diradical **3**, a stable organic magnetic molecule consisting of two spin-containing fragments linked by a nitrogen atom, is reported. Electron paramagnetic resonance (EPR) analysis in methyltetrahydrofuran solution ($\sim 10^{-3}$ M) at low temperatures showed a typical fine structure ($g_{xx}=2.0042$; $g_{yy}=2.0048$; $g_{zz}=2.0027$) of $\Delta m_s=\pm 1$ transition ($|D/hc|=0.0071$ cm^{-1}; $|E/hc|=0.0006$ cm^{-1}) as well as a broad ($\Delta H_{pp}=7.5$ G) and weak signal of $\Delta m_s=\pm 2$ transition ($g=4.124$), due to an asymmetric and excited triplet state corresponding to an intramolecular spin–spin interaction which diminishes with decreasing temperature. It also showed a pair of small peaks, that might be associated with a weaker dipole–dipole interaction which diminishes with increasing temperature, emerging at both sides of a central and single peak due to a doublet state resonance corresponding to 2,2′,2″,4′,4″,6,6′,6″-octachloro-4-{3,5-dichloro-4-[bis(2,4,6-trichlorophenyl)methylene]cyclohexa-2,5-dienylideneamino}triphenylmethyl radical **4**, obtained by smooth oxidation of **3**. From magnetic susceptibility measurements of the sample in the solid, a linear four-spin model was applied to establish that the singlet is the ground state of the molecule and that two triplets ($J_{intra}=-286\pm 30$ K, $J'_{inter}=-160\pm 50$ K) were the low-lying excited states. Organic solutions of **3** in air slowly oxidize to give **4**, a much more persistent monoradical which is also obtained by a smooth oxidation of **3** with $AgNO_3$ in $CHCl_3$. Cyclic voltammograms for the reduction of **3** and **4** in dimethylformamide (DMF) with tetra-*n*-butylammonium perchlorate exhibited three consecutive redox couples with standard potentials of −0.23, −0.58 and −0.74 V *vs.* SCE, indicating a reasonable stability of anions $\mathbf{3}^{\cdot -}$ and $\mathbf{3}^{2-}$ in DMF solution.

There is great current interest in the preparation of organic molecular materials with new magnetic properties.[1] Organic molecules with paramagnetic behavior are those with open-shell electronic structures where one or more electrons are unpaired. These molecules are called radicals or polyradicals, and they are normally transient and very reactive to air, moisture and, in general, to their environment. Thus, if free radicals are to be good candidates for magnetic materials, it has to be possible to prepare, handle and store them without difficulty. The stability of the carbon-centered radicals is mainly achieved by steric protection.[2,3]

In highly chlorinated triphenylmethyl radicals, this protection is mainly accomplished by the six aromatic chlorines in the *ortho*-positions surrounding the trivalent carbon atom.[3] Thus, this kind of very stable free radical is completely unassociated in crystalline solids with no appreciable decomposition either in solid or in solution. The synthesis of new polyradical molecules of great persistence and their physical properties involving magnetic behavior have recently been published.[4,5]

The preparation of radical amino **1**,[6] a new polychlorotriphenylmethyl radical of the TTM [tris(2,4,6-trichlorophenyl)-methyl] series, as a potential radical intermediate in the synthesis of many new polyradicals which use the characteristics and extensive reactivity of the amino group, has also recently been published. The isolation of a secondary reaction product which could be identified, from preliminary analysis results, as a secondary amine, resulting from the condensation of two molecules of the hydrocarbon salt **2**[5a] with ammonia followed by reduction with $SnCl_2$, was also mentioned.[6]

It is now possible to fully describe this new secondary amine as a diradical of the TTM series, the amino-diradical **3**, whose two spin-bearing moieties, the triphenylmethyl radicals, are held together by the amine function, bonded in the *para*-position of a phenyl of each moiety. The radical **3** is easily oxidized in solution to a new and very persistent paramagnet, the imino-radical **4**.

Lahti *et al.* have carried out semi-empirical calculations to

predict the ground state spin multiplicity of a large number of systems composed of two doublets, organic oxyl radicals, or two triplets, methylenes or organic nitrenes, connected by a spacer consisting of a magnetic coupling unit.[7] When the spacer is a heteroatom,[7b] oxygen or nitrogen, they predicted an antiferromagnetic coupling in the *para,para′* connectivity, that was stronger with a nitrogen atom as spacer than with an oxygen atom. In non-planar geometries, this interaction dropped substantially to give nearly degenerate high-spin and low-spin in the ground-state.

In Lahti's terminology, the magnetic material **3** consists of two spin-containing (SC) fragments, two carbon-centered radicals, connected by a two-electron one-center heteroatom π spacer, a nitrogen atom. Due to the relative stability of **3**, described below, its properties could be tested and the predictions regarding the multiplicity of its electronic ground-state corroborated.

Results

The reaction of the hydrocarbon salt **2**[5a] with an excess of ammonia in CH_2Cl_2 followed by treatment with $SnCl_2$ gave the amino-radical **1**[6] (58%), the diradical **3** (17%) and a low yield of the TTM radical[8] (9%) as a direct reduction of salt **2** (Scheme 1). The amino-diradical **3** is a green microcrystalline solid with a visible spectrum in cyclohexane as follows: λ/nm (ε/dm^3 mol^{-1} cm^{-1}), 375 (40 600), 440 (15 200), 633 (17 700). It is stable in the solid state (its decomposition in 13 d in air is practically nil, checked by electronic spectroscopy), and it oxidizes in solution to the more persistent imino-radical **4**.

A smooth oxidative treatment of **3** with a basic aqueous solution of silver nitrate in chloroform gave **4** quantitatively, which, by the action of $SnCl_2$ in tetrahydrofuran, reverted to **3**. Radical **4** is an extremely persistent dark brown solid, even in solution and in the dark. Its visible spectrum in cyclohexane is as follows; λ/nm (ε/dm^3 mol^{-1} cm^{-1}), 377 (37 350), 409 (29 400), 573 (15 100), 619 (12 700).

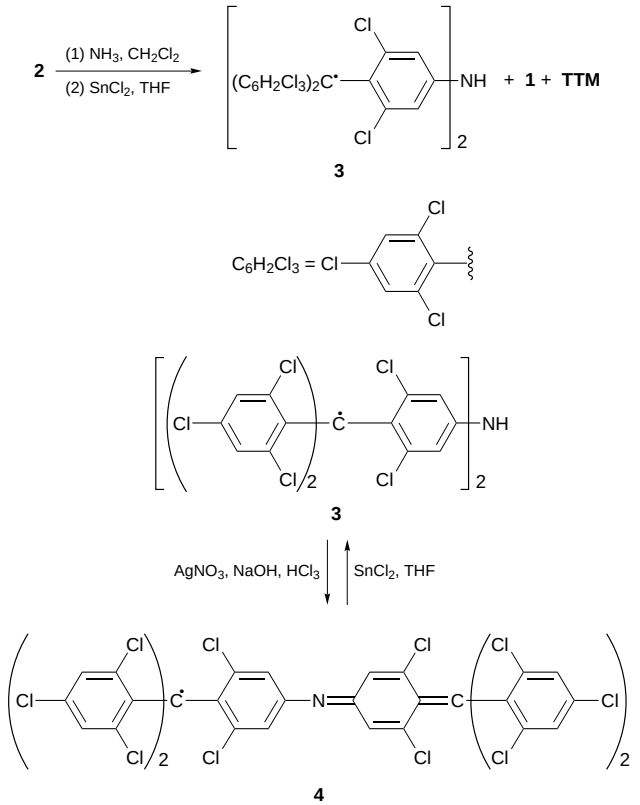

Scheme 1

Cyclic voltammetry (CV)

A cyclic voltammogram for the reduction of a solution of 0.5 mM amino-diradical **3** in dimethylformamide (DMF) with 0.1 M tetra-*n*-butylammonium perchlorate (TBAP) is presented in Fig. 1. In the potential range between 0 and −1.2 V three consecutive redox couples, O_1/R_1, O_2/R_2 and O_3/R_3, with respective standard potentials E^0 of −0.23, −0.58 and −0.74 V *vs.* SCE (NaCl-saturated calomel electrode) can be observed. No more peaks were found for **3** at potentials higher than −1.2 V. The above redox couples were also recorded in the cyclic voltammograms of a saturated solution of the imino-radical **4** in DMF (Fig. 2), along with a further irreversible peak R_4. The different height of the peaks in Fig. 1 and 2 is due to the lower concentration of **4** than **3**, whereas the presence of the additional peak R_4 in Fig. 2 can be ascribed to reaction of **4** with electrogenerated radicals at the electrode reaction layer. Fig. 1 also shows that O_2/R_2 and O_3/R_3 couples partially overlapped, and for this reason the height of peaks R_2, R_3 and O_2 cannot be accurately determined. In fact, the O_1R_1, O_2/R_2 and O_3/R_3 couples behaved as reversible one-electron systems controlled by diffusion. So the differences between the anodic and cathodic peak potentials ($E_p^a - E_p^c$) for each of these three couples was close to 60 mV in all scan rates (v) considered, whereas the height of peaks R_1, R_2+R_3,

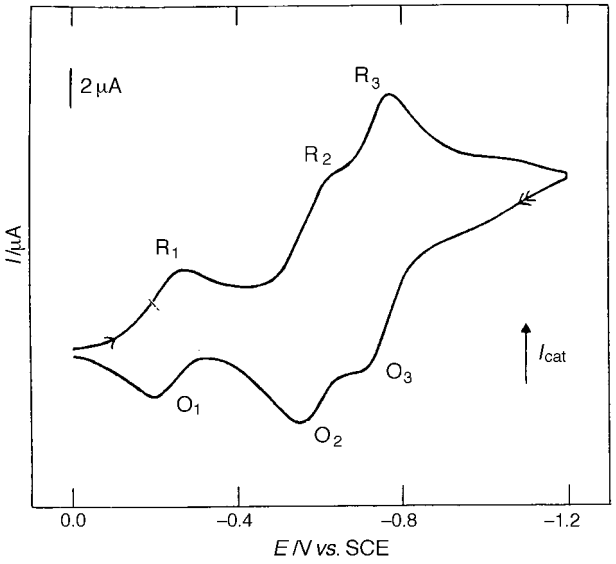

Fig. 1 Cyclic voltammogram of a 0.5 mM amino-radical **3** solution in 0.1 M TBAP+DMF. Scan rate 50 mV s^{-1} and temperature 25 °C. Starting and final potential 0 V; reverse potential −1.2 V.

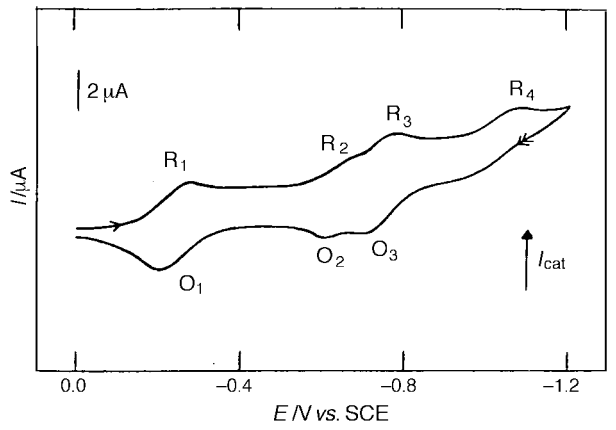

Fig. 2 Cyclic voltammogram of a saturated imino-radical **4** solution in 0.1 M TBAP+DMF under the same experimental conditions as indicated in Fig. 1

O_1 and O_2+O_3 increased linearly with the square root of the scan rate.[9] Note that the height of peaks R_2+R_3 was approximately equal to that of peaks O_2+O_3 and twice that of peak R_1. However, the $|I_p^a|/I_p^c$ ratio (I_p^a = anodic peak current, I_p^c = cathodic peak current) for the O_1/R_1 pair was *ca.* 0.6 (Fig. 1).

The CV behavior for **3** described above helps to establish that the O_1/R_1 couple corresponds to the equilibrium reaction between the imino-radical **4** and the amino-diradical **3**, *i.e.* eqn. (1),

$$\mathbf{4} + H^+ + 1\,e^- \rightleftarrows \mathbf{3} \quad (1)$$

where H^+ proceeds from a proton donor such as water, always present in small amounts in DMF. The O_2/R_2 pair can then be ascribed to the reversible conversion of **3** into its radical-anion $\mathbf{3}^{\cdot -}$: eqn. (2),

$$\mathbf{3} + 1\,e^- \rightleftarrows \mathbf{3}^{\cdot -} \quad (2)$$

and the O_3/R_3 couple to the equilibrium (3) between $\mathbf{3}^{\cdot -}$ and its dianion $\mathbf{3}^{2-}$.

$$\mathbf{3}^{\cdot -} + 1\,e^- \rightleftarrows \mathbf{3}^{2-} \quad (3)$$

The presence of three consecutive reversible one-electron redox pairs for compound **3** (Scheme 2) indicates a good stability of anions $\mathbf{3}^{\cdot -}$ and $\mathbf{3}^{2-}$ in DMF, without the existence of any chemical reaction involving their disappearance from the medium.

In addition, the small difference between the second and third cathodic peaks (160 mV) in **3** is a measure of the small interactions between the two negative charges in the dianion $\mathbf{3}^{2-}$, which must be situated apart from each other to prevent Coulombic repulsions between them. By analogy with the electronic structure in the neutral radical, in $\mathbf{3}^{2-}$ the charges will be located mainly in the aliphatic carbon atoms of each triphenylmethyl moiety adopting a stable conformation far from coplanarity, due to the presence of the six *ortho*-chlorines in the phenyl rings. The stability of $\mathbf{3}^{2-}$ is then mainly attributed to steric protection.

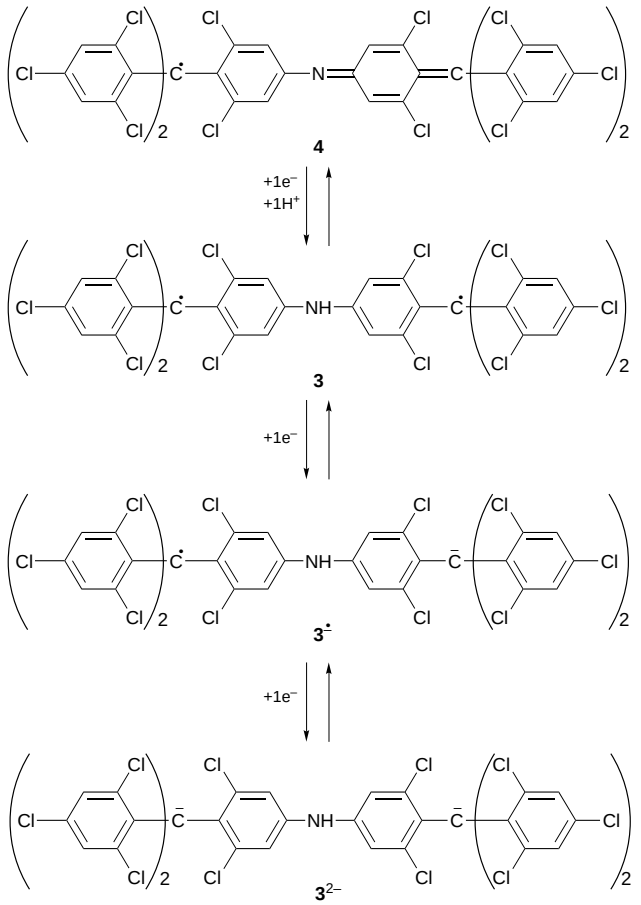

Scheme 2

As shown in Fig. 2, a saturated solution of **4** in DMF with TBAP (0.1 M) displayed the same O_1/R_1, O_2/R_2 and O_3/R_3 pairs as **3**. In this case, the height of peaks R_2+R_3 is only 1.4 times that of peak R_1. In addition, the $|I_p^a|/I_p^c$ ratio for the corresponding O_1/R_1 couple was *ca.* 1 in all v tested, as expected if all amino-diradical **3** formed in peak R_1 is also oxidized to imino-radical **4** in peak O_1. The height of peaks R_1 and O_1 for compound **4** in a given v value was similar to that of peak O_1 found for compound **3**. Since these peaks are diffusion-controlled, their heights must be proportional to the solubility of **4**, *i.e.* its concentration in the saturated solution. This suggests that the $|I_p^a|/I_p^c$ ratio of *ca.* 0.6 found for the O_1/R_1 couple of compound **3** (Fig. 1) is due to the loss of compound **4** near the electrode towards the bulk solution during the oxidation of **3** in peak O_1 until reaching its saturation in the reaction layer. So, by comparing the height of the diffusion-controlled peak R_1 for compounds **3** and **4**, which must be directly proportional to their concentrations, the solubility of **4** in DMF was found to be 0.31 mM.

The presence of peak R_4 in Fig. 2 is more difficult to explain. This irreversible peak has a height similar to that of peak R_1, which means it is diffusion-controlled. In addition, the difference between its cathodic half-peak and peak potentials, $(E_{p/2}^c - E_p^c)$, was 70–80 mV, whereas its E_p^c value varies linearly with $-\log v$ with a slope close to 30 mV per decade. All these parameters agree with the behavior expected for a first-order one-electron EC mechanism [theoretical values at 25.0 °C:[9] $(E_{p/2}^c - E_p^c) = 59.6$ mV, slope of E_p^c *vs.* $-\log v$ plot = 29.6 mV per decade].

The fact that the height of peaks R_2+R_3 in Fig. 2 is significantly lower than twice that of peak R_1, indicates that not all of the compound **3** formed in this last peak is completely converted into $\mathbf{3}^{\cdot -}$ and $\mathbf{3}^{2-}$, *i.e.* part of these ions disappears at the reaction layer. This phenomenon is not observed in cyclic voltammograms of **3** (Fig. 1) and suggests a reaction of $\mathbf{3}^{\cdot -}$ and $\mathbf{3}^{2-}$ with **4**, present in the reaction layer by its diffusion from bulk solution, yielding the electroactive species of peak R_4. A reversible one-electron reduction of this species, followed by an irreversible chemical decomposition of the resulting compound, could explain the EC process found for this peak.

Electron paramagnetic resonance (EPR)

Recently, the X-band EPR spectrum of the amino-radical **1** recorded in CH_2Cl_2 solution at 173 K was reported.[6] It displayed an overlapping triplet of septets, centered at $g = 2.0030$, corresponding to the hyperfine splitting of the free electron with the nitrogen atom ($a_N = 1.10$ G) and the six aromatic *meta*-hydrogens ($a_H = 1.10$ G). The magnetic interaction with the α-amino hydrogen ones gave negligible splitting and most probably contributes to line broadening.

The spectrum found for the isotropic solution ($\sim 10^{-3}$ M) of amino-diradical **3** in 2-methyltetrahydrofuran (MTHF) at room temperature contained a single broad line centered at $g = 2.0036$ with a peak-to-peak linewidth of the derivative line, $\Delta H_{pp} = 6.2$ G. This large linewidth value and the existence of abnormally intense tails in the derivative line, which increase with decreasing temperature, are accounted for by the modulation of the energies of the triplet spin levels due to the anisotropic part of the intramolecular electron–electron magnetic interaction. These large absorptions probably hamper the observation of satellite lines corresponding to the coupling with ^{13}C nuclear spins of carbons in the molecule, mainly those from α-carbons where the majority of the spin density resides,[10] and preclude any information in fluid solution about the strong or weak electron–electron exchange coupling (the scalar part of the magnetic interaction between two unpaired electrons) which will be expressed by a normal or a half value of those coupling constants, respectively.[11]

At low temperatures ($\sim$150 K), in a very viscous solution near to glassy MTHF, the spectrum showed three pairs of lines in the $\Delta m_s = \pm 1$ region (Fig. 3), typical of a randomly oriented ensemble of immobilized triplet species without axial symmetry, described by the zero-field splitting parameters $|D/hc| = 0.0071$ cm^{-1} and $|E/hc| = 0.0006$ cm^{-1}, with the principal values of the g tensor being $g_{xx} = 2.0032$, $g_{yy} = 2.0037$ and $g_{zz} = 2.0029$. Further confirmation of the triplet state configuration was provided by the observation of the $\Delta m_s = \pm 2$ region of a broad line centered at $g = 4.124$, with a peak-to-peak spacing, $\Delta H_{pp} = 7.5$ G (Fig. 3). Although the fine structure in the $\Delta m_s = \pm 1$ remains at lower temperatures in the rigid glass MTHF, the intensity rapidly decreases with decreasing temperature, being hardly detected at temperatures lower than 70 K, which is consistent with the fact that the triplet is an excited state. In addition, an intense central line corresponding to $S = 1/2$ species ($g = 2.0032$) appears, which can be ascribed to the imino-radical **4** always present in the sample as an impurity, resulting from the smooth oxidation of amino-diradical **3**. From parameter D, the average distance between the two unpaired electrons has been estimated[12] as 7.15 Å, a smaller value than the theoretical one of 9.1 Å.[13]

At lower temperatures and in conditions of microwave saturation of the doublet state resonance (power: 5.02 mW), a pair of signals ($g = 2.0034$) emerging from the edges of the central line in the region $\Delta m_s = \pm 1$ appears. In Fig. 4, the spectrum recorded at 90 K shows the presence of both interactions, the strong one with a fine structure of three pairs of lines of low intensity and the weak one with a closer pair of lines emerging from the wings of the strong single line. In Fig. 5, a series of spectra recorded from 4 to 90 K, irradiating the sample at low microwave power (0.2 mW) in conditions of non-saturation of these lateral signals is displayed. In this series, while the intensity of the lateral signals diminishes from 4 K upwards, in such a way that they practically disappear at 59 K, the intensity of the central signal increases from 4 to 90 K, due to microwave saturation of the doublet state resonance. At much lower microwave power (10^{-3} mW), the intensity of the central line gradually decreases from 4 K upwards, following Curie's law in the temperature range 37–90 K, where the signal amplitude is inversely proportional to the temperature (Fig. 6). So, both signals, the doublet and the central single line, must correspond to different species, as shown by selective microwave saturation, and the idea that the doublet might correspond to a weak ferromagnetic interaction in the ground state between pairs of molecules, since its intensity increases with decreasing temperature is not discarded.

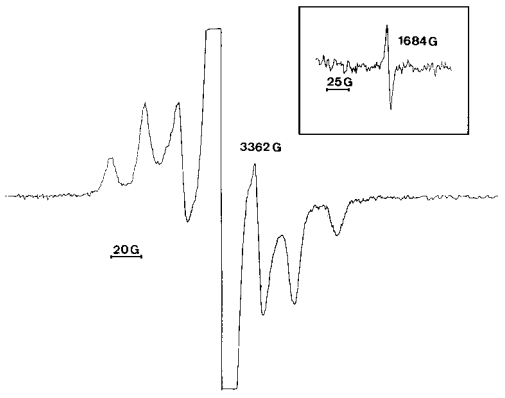

Fig. 3 EPR spectrum of **3**; $\Delta m_s = \pm 1$ transition in MTHF glass at 150 K. Insert shows the signal corresponding to $\Delta m_s = \pm 2$ forbidden transition

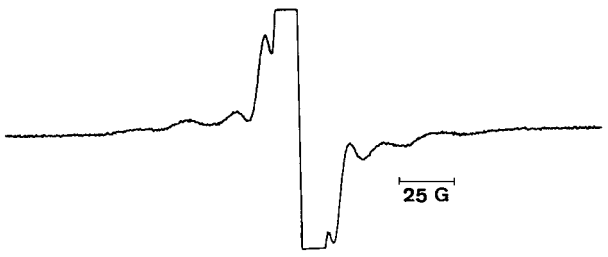

Fig. 4 EPR spectrum of **3**; $\Delta m_s = \pm 1$ transition in MTHF glass at 90 K, showing the presence of the two dipole–dipole interactions, as explained in the text

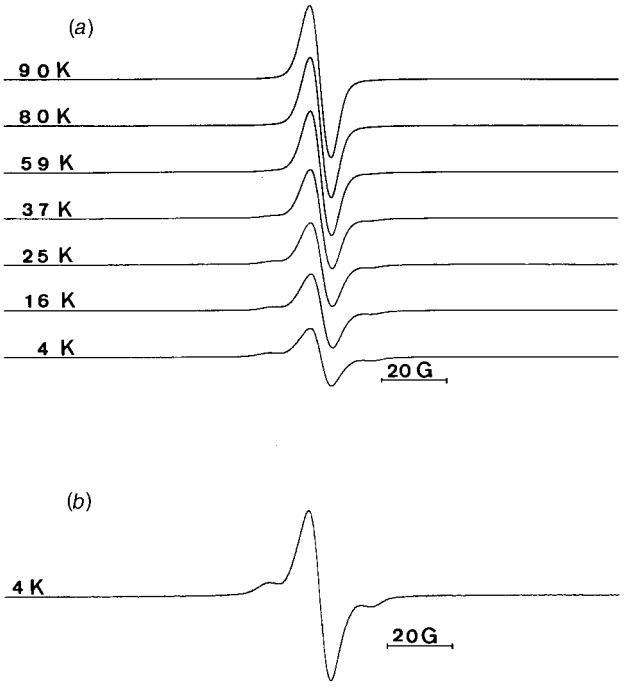

Fig. 5 (*a*) A series of EPR spectra of a solution of **3** in MTHF glass from 4 to 90 K (microwave power, 0.2 mW), showing the intensity dependence of the weak dipole–dipole interaction as explained in the text, and (*b*) the EPR spectrum at 4 K

The EPR spectrum of imino-radical **4** in tetrachloroethylene solution at room temperature consisted of a single line, $\Delta H_{pp} = 2.6$ G, centered at $g = 2.0037$ [Fig. 7(*a*)]. At higher gain, the isotropic coupling with the ^{13}C nuclear spins of the α-carbon atoms in the molecule appeared in the spectrum with a coupling constant, $a \approx 15$ G. This value is practically half the value corresponding to the ^{13}C hyperfine coupling in radicals of the TTM series[5a,c,6] ($a \approx 29.5$ G), which indicates that the spin density on these carbons is also half the normal value and, consequently, the electronic structure of **4** can be depicted

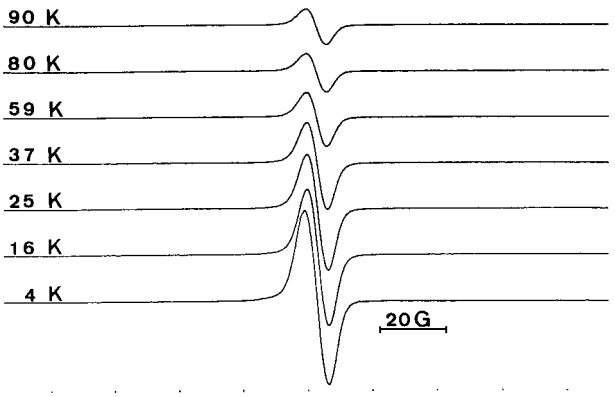

Fig. 6 A series of EPR spectra of a solution of **3** in MTHF glass from 4 to 90 K (microwave power, 10^{-3} mW), showing the normal intensity dependence of the doublet state resonance, as explained in the text

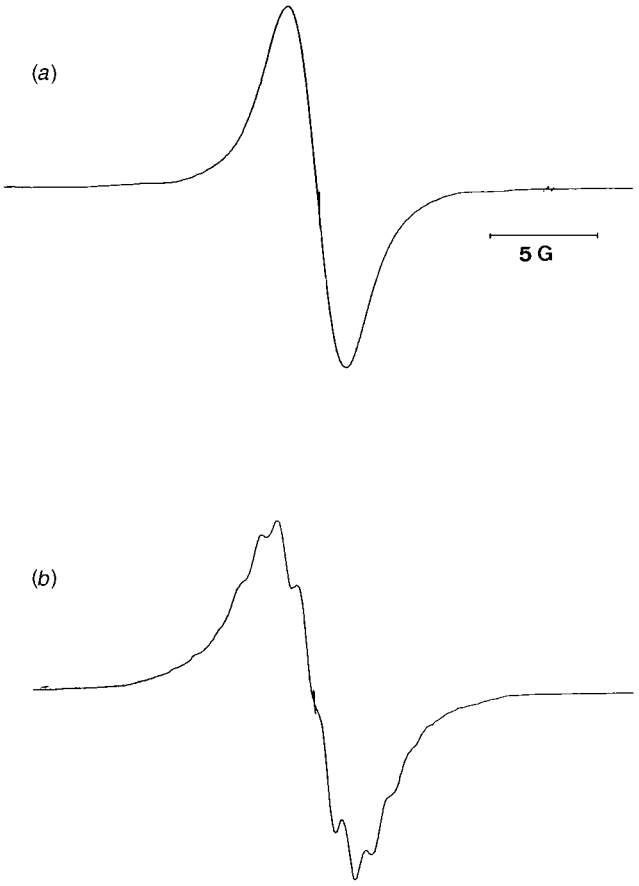

Fig. 7 EPR spectrum of **4** (*a*) in tetrachloroethylene at room temperature and (*b*) in CH_2Cl_2 at 213 K

as a structure in resonance between the two canonical structures shown in Scheme 3.

A hyperfine splitting of an overlapping multiplet of lines appeared in the spectrum when recorded in CH_2Cl_2 at low temperatures (213 K and lower) [Fig. 7(*b*)].

Magnetic susceptiblity

The molar magnetic susceptibility (χ_S) of diradical **3** was measured in two different samples in the temperature range 4–300 K, one of them with a SQUID magnetometer and the other one with a Faraday balance operating in a field-strength of 20 and 17 kOe, respectively. The data ($\chi'_S=\chi_S-\chi_{dia}-\chi_{holder}$) were corrected for the magnetization of the sample holder and for the diamagnetic susceptibility of the molecule (-608.7×10^{-6} cm^3 mol^{-1}, using Pascal's constants). The thermal variation of the molar effective magnetic moment in Bohr magnetons shown in Fig. 8 is given by $\mu_{eff}=2.828(\chi'_S T)^{1/2}$.

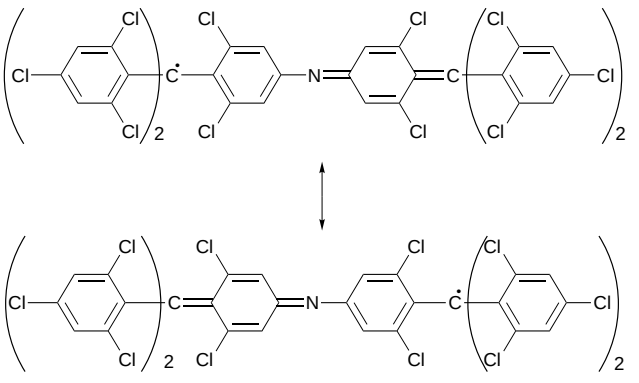

Scheme 3

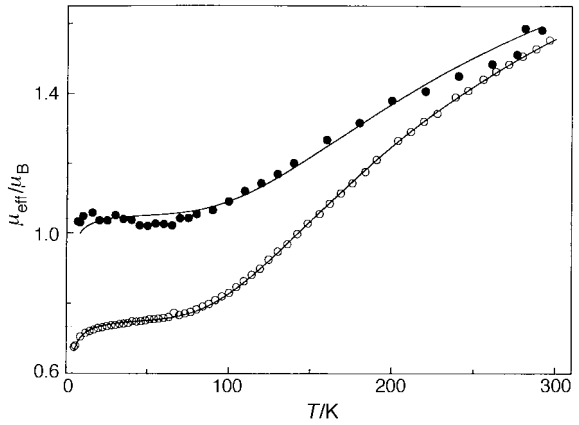

Fig. 8 Thermal variation of μ_{eff}/μ_B for amino-diradical **3** (●) from sample measured in a Faraday balance operating with a field-strength of 17 kOe and (○) from sample measured in a SQUID magnetometer operating with a field-strength of 20 kOe. The solid lines are theoretical ones, as described in the text.

As shown in Fig. 8, when the temperature decreases from 300 K, the μ_{eff} value of both microcrystalline samples decreases continuously. This behavior is associated with a strong antiferromagnetic interaction. In the range 12–75 K, there is a plateau of $\mu_{eff}=0.73$ and $\mu_{eff}=1.04$ μ_B for the two samples, respectively, which suggests that some monoradical impurities exist in greater proportions in one of the samples.

After applying different models to account for these results, the model which best fits the experimental data is of a system composed of a couple of diradical molecules with an intramolecular interaction characterized by J, interacting with each other at a strength given by J' (Fig. 9).[14] In such a system, there is a proportion of monoradical impurities, most probably the oxidized imino-radical **4**, which differs from one sample to the next.

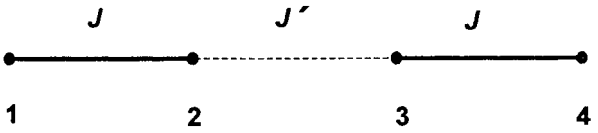

Fig. 9 Model system for diradical interaction

The spin Hamiltonian for such a system is given by eqn. (4),

$$H=-2J\boldsymbol{S}_1\boldsymbol{S}_2-2J'\boldsymbol{S}_2\boldsymbol{S}_3-2J\boldsymbol{S}_3\boldsymbol{S}_4 \quad (4)$$

where $\boldsymbol{S}_i$ corresponds to the spin angular momentum vector for the single electron in each center.

The total spin states and energies, λ_i, corresponding to this system are obtained from the diagonalization of the Hamiltonian [eqn. (5)]

$$\begin{aligned}
&\text{Quintuplet (S = 2)} \quad \lambda_1=-J-\frac{J'}{2}\\
&\text{Triplet (S = 1)} \quad \lambda_2=J-\frac{J'}{2}\\
&\text{Triplet (S = 1)} \quad \lambda_3=\frac{J'}{2}+\sqrt{J'^2+J^2}\\
&\text{Triplet (S = 1)} \quad \lambda_4=\frac{J'}{2}-\sqrt{J'^2+J^2}\\
&\text{Singlet (S = 0)} \quad \lambda_5=\frac{J'}{2}+J+2\sqrt{\left(\frac{J'}{2}\right)^2-\frac{J'}{2}J+J^2}\\
&\text{Singlet (S = 0)} \quad \lambda_6=\frac{J'}{2}+J-2\sqrt{\left(\frac{J'}{2}\right)^2-\frac{J'}{2}J+J^2}
\end{aligned} \quad (5)$$

The expression for the susceptibility, using the van Vleck

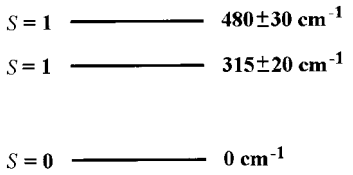

Fig. 10 Diagram of levels for the singlet ground state and two triplet excited states

formula,[15] is as in eqn. (6),

$$\chi_d = \frac{\chi_D}{2} = \frac{N\mu_B^2 g^2}{6k_B T} \times \frac{30\,e^{-\beta_1} + 6\,e^{-\beta_2} + 6\,e^{-\beta_3} + 6\,e^{-\beta_4}}{5\,e^{-\beta_1} + 3\,e^{-\beta_2} + 3\,e^{-\beta_3} + 3\,e^{-\beta_4} + e^{-\beta_5} + e^{-\beta_6}} \quad (6)$$

where: $\beta_i = \lambda_i/k_B T$, N is the Avogadro number, μ_B is the Bohr magnetron, g is the Landé factor, k_B is the Boltzmann constant, χ_D is the susceptibility of a cluster compound of two diradical molecules and χ_d is the susceptibility per molecule.

The expression for the susceptibility of the monoradical impurity is eqn. (7).

$$\chi_M = \frac{N\mu_B^2 g^2}{4k_B T} \quad (7)$$

Then, the thermal dependence of μ_{eff} for the whole system becomes as in eqn. (8),

$$\mu_{eff}/\mu_B = 2.828 \times \sqrt{\frac{TF_m}{T-\theta_m}\frac{3}{8} + (1-F_m)\frac{T}{T-\theta_d}} \times \frac{15\,e^{\beta_1} + 3\,e^{-\beta_2} + 3\,e^{-\beta_3} + 3\,e^{-\beta_4}}{10\,e^{-\beta_1} + 6\,e^{-\beta_2} + 6\,e^{-\beta_3} + 6\,e^{-\beta_4} + 2\,e^{-\beta_5} + 2\,e^{-\beta_6}} \quad (8)$$

assuming $g=2$, where: F_m is the fraction of monoradical impurity and $(1-F_m)=F_d$ is the fraction of diradical molecules and θ_m and θ_d account for the effect of residual path interactions among molecules which are not considered in the model.

This equation was fitted to the experimental data obtained for both samples to give the following parameters: (*a*) from sample analyzed in the SQUID: $F_m = 0.19 \pm 0.02$; $F_d = 0.81 \pm 0.02$; $\theta_m = -1.50 \pm 0.5$ K; $\theta_d = -1 \pm 1$ K; $J = -290 \pm 20$ K; $J' = -203 \pm 40$ K; (*b*) from sample analyzed in the Faraday balance: $F_m = 0.37 \pm 0.02$; $F_d = 0.63 \pm 0.02$; $\theta_m = -1.1 \pm 0.8$ K; $\theta_d = -1 \pm 1$ K; $J = -296 \pm 30$ K; $J' = -160 \pm 50$ K. The values of J and J' are quite similar for both samples although they display different impurity content.

The diagram of levels for the singlet ground state, λ_6, and the first two triplet excited states of the system, the lowest triplet λ_4 and the next λ_2 considering the above values for J and J' and their intervals of error, can be established as shown in Fig. 10.

The highest excited states, one singlet, one triplet and one quintuplet, the three of energy too high to be significantly populated in the normal range of temperatures, are not considered. The low negative values for θ_m and θ_d indicate the existence of small residual antiferromagnetic interactions among molecules.

Discussion

Amino-diradical **3** is a clear and stable example of a system composed of two spin-bearing units linked by a two-electron one-center heteroatom π spacer. Both the EPR analysis and the results from magnetic susceptibility measurements predict a strong dipole–dipole interaction, either in dilute solution (EPR) or in the solid (susceptibility), which is attributed to the intramolecular electron spin–spin interaction, splitting the spin states of the molecule into a ground state singlet and an excited triplet. On the other hand, weaker interactions either in the glassy solution or in the solid state are also predicted by EPR and susceptibility measurements, respectively. At present, we are not able to attribute the first one which increases with decreasing temperature, but the second one is ascribed to an intermolecular antiferromagnetic interaction.

Concerning the intramolecular interaction, Lahti *et al.* predicted, by using AM1-CI semi-empirical procedures, a strongly antiferromagnetic coupling in the *para*,*para'* connectivity in this kind of system in their planar conformation, with a dominant closed-shell configuration in their ground state, best described by a pair of equivalent zwitterionic Kekulé resonance structures.

All these predictions are confirmed in amino-diradical **3**. Results from EPR analysis and susceptibility measurements, as shown above, established the singlet character of the ground state of **3**, which is best described as a resonance of the canonical structures shown in Scheme 4.

However, the remarkable persistence of polychlorotriphenylmethyl radicals is mainly attributed to steric shielding by the six chlorines surrounding the trivalent carbon, which leads to a torsion of the phenyl rings around their bond with the central carbon. As a result, these radicals adopt a stable propeller-like conformation with a significant inhibition of the delocalization of the free electron into the three rings. In the stable non-planar conformation most of the spin density is in the central carbon.

These findings suggest that in amino-diradical **3**, the diradical structure plays an important role in the configuration of its ground state if the twisted geometry is the most stable conformation, with the free electron mainly confined to the central carbon atom of each triphenylmethyl moiety. In such a case, the dipolar spin–spin interaction is much weaker than in the planar conformation, as also predicted by Lahti *et al.*,[7b] and the triplet–singlet energy gap is not very high, 1.38 kcal mol^{-1} (1 cal = 4.184 J) as stated above.

On the other hand, the fact that the average distance between the unpaired electrons is smaller than the theoretical one, as described in the EPR section, favours the closed-shell electronic structures, where the molecule is forced to adopt a more planar conformation between the two α-carbons. These conformations make the delocalization of the electronic spin on the phenylene rings easier than on the four extreme phenyls.

Concerning the intermolecular interaction in the solid state, it is obvious that the proposed model of a weak interacting dimer from magnetic susceptibility measurements can only provide a simplified picture of the real situation, but it does involve enough radical centers and interactions among them to reproduce the low lying energy terms with sufficient accuracy. If the detailed treatment of the interactions with other radical centers (*e.g.* the tendency to form a linear chain) is

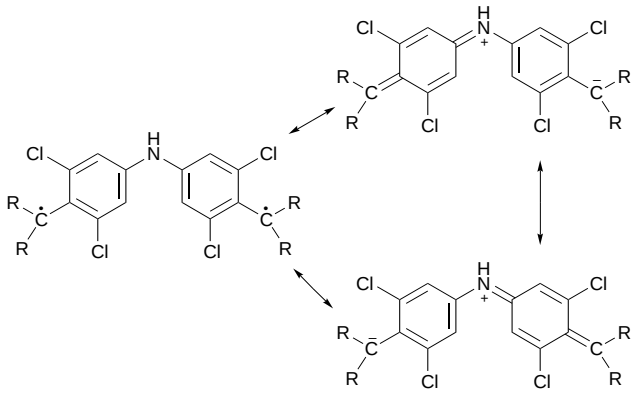

Scheme 4

included in the model, neither the spin multiplicity of the three low-lying levels varies nor the energy values change significantly.

So, it can be concluded that a ground singlet state with a total pairing of the spins and, at least, two triplets as the nearest excited states, is the low-lying energy diagram which achieves a good fit of the experimental data for amino-diradical **3** in the solid state.

Experimental

General procedures

All melting points are uncorrected. Solvents were dried and purified before use. THF was freshly distilled from sodium benzophenone ketyl. Magnetic susceptibility data for microcrystalline samples of amino-diradical **3** were measured from 4 to 298 K with a Manics DSM8 susceptometer operating with a field strength of 17 kOe and with a SQUID magnetometer operating with a field strength of 20 kOe.

Electrochemical measurements

The cyclic voltammetric experiments were carried out in a three-electrode cell under an argon atmosphere. A platinum sphere with a surface area of 0.093 cm^2 was used as the working electrode and a Pt wire as the counter electrode. The reference electrode was an SCE (NaCl-saturated aqueous solution) connected to the cell through a salt bridge containing a 0.1 M TBAP–DMF solution. The temperature of test solutions and of the SCE was kept at 25 °C. In all experiments, the cell was maintained in darkness to avoid the photochemical decomposition of substrates in solution.

CV measurements were performed with standard equipment consisting of a PAR 175 universal programmer, an Amel 551 potentiostat and a Philips 8043 X-Y recorder. Cyclic voltammograms of all solutions were recorded at a scan rate (v) of 20–200 mV s^{-1}.

A solution of amino-diradical **3** (0.5 mM) in DMF containing TBAP (0.1 M) as the background electrolyte was studied. Since imino-radical **4** showed lower solubility in DMF, its CV measurements were carried out using a saturated solution in DMF with TBAP (0.1 M). The volume of all test solutions was 25 ml.

EPR experiments

EPR spectra were recorded with a Varian E-109 spectrometer working in the X band and using a Varian E-257 temperature-controller to obtain spectra at temperatures as low as 130 K. A Bruker ESP 300 spectrometer with a Bruker ER 4112 HV continuous-flow liquid helium cryostat and an Oxford Instruments temperature-controller system was used to obtain EPR spectra at lower temperatures (4 K). Samples of amino-diradical **3** and imino-radical **4** were prepared in quartz EPR tubes and degassed by three freeze–pump–thaw cycles before being inserted into the EPR cavity. Handling of radicals in solution was performed in the dark.

Tris(2,4,6-trichlorophenyl)carbenium hexachloroantimonate 2

$SbCl_5$ (1.5 ml) was slowly added to a solution of tris(2,4,6-trichlorophenyl)methyl radical[8] (1.80 g) in CCl_4 (240 ml), and the mixture was left at room temperature under an argon atmosphere for 24 h. The precipitate was filtered, washed with CCl_4 and dried, and identified as salt **2** (2.78 g; 96%), dark blue crystals mp 183–185 °C (lit.[5a] mp 180–182 °C).

4-Amino-2,2′,2″,4′,4″,6,6′,6″-octachlorotriphenylmethyl radical 1 and 4,4-iminobis(2,2′,2″,4′,4″,6,6′,6″-octachlorotriphenylmethyl) diradical 3

Dry NH_3 was passed slowly in the dark, through a solution of salt **2** (2.12 g) in CH_2Cl_2 (500 ml) until the blue color of the solution suddenly changed to red. Then argon was passed through to eliminate the NH_3 and the resulting mixture was filtered. The filtrate was evaporated to dryness and the red residue was dissolved in THF (100 ml). Anhydrous $SnCl_2$ (0.56 g) was added to the solution, and the mixture was stirred in the dark at room temperature for 30 min. The resulting mixture was filtered and evaporated to dryness. The residue in diethyl ether (100 ml), washed with aqueous $NaHCO_3$ and with water, then dried and evaporated, gave a new residue which was chromatographed (silica gel flash chromatography, CCl_4–$CHCl_3$, 1:1) to give the following: (*a*) radical **1** (0.26 g; 9%) identified by mp and IR. (*b*) Amino-diradical **3** (0.14 g; 17%), mp 268–271 °C; ν/cm^{-1} (KBr) 3400 (w), 3100 (w), 1565 (s), 1525 (m), 1370 (m), 1310 (m), 1180 (m), 1130 (m), 1075 (w), 1055 (w), 980 (w), 920 (w), 850 (m), 820 (m), 805 (m), 790 (m); UV–VIS (cyclohexane) λ_{max}/nm (ε/dm^3 mol^{-1} cm^{-1}) 375 (40 600), 440 (15 200), 633 (13 700). Anal. Calc. for $C_{38}H_{13}Cl_{16}N$: 43.4; H, 1.25; N, 1.3; Cl, 54.0. Found: C, 43.9; H, 1.4; N, 1.3; Cl, 53.9%. (*c*) Radical TTM (0.74 g; 58%), identified by its mp and IR.

Oxidation of 3. Synthesis of 2,2′,2″,4′,4″,6,6′,6″-octachloro-4-{3,5-dichloro-4-[bis(2,4,6-trichlorophenyl)methylene]cyclohexa-2,5-dienylidenamino}triphenylmethyl radical 4

To a solution of **3** (20 mg) in $CHCl_3$ (5 ml) at room temperature was added a basic aqueous solution of $AgNO_3$ (5 ml, $AgNO_3$ 2%, NaOH 2%) and the resulting mixture was vigorously stirred for 5 min in the dark. The organic solution was washed with water, dried and evaporated to dryness, giving a residue which was chromatographed (silica gel, $CHCl_3$) to give **4** (18 mg; 90%), mp > 350 °C; ν/cm^{-1} (KBr) 3080 (w), 1550 (s), 1530 (s), 1370 (s), 1285 (w), 1180 (m), 1130 (s), 1075 (w), 960 (w), 920 (w), 885 (w), 850 (s), 820 (m), 800 (s), 785 (s); UV–VIS (cyclohexane) λ_{max}/nm (ε/dm^2 mol^{-1} cm^{-1}) 210 (128 000), 376 (37 000), 413 (31 000), 573 (15 000), 621 (12 000). Anal. Calc. for $C_{38}H_{12}Cl_{16}N$: C, 43.5; H, 1.1; N, 1.3; Cl, 54.0. Found: C, 43.0; H, 1.1; N, 1.3; Cl, 54.3%.

Reduction of 4 to give 3

Anhydrous $SnCl_2$ (5 mg) was added to a solution of **4** (20 mg) in $CHCl_3$ (5 ml) and the mixture was vigorously stirred at room temperature and in the dark (30 min). Then, the solvent was evaporated off and the residue in $CHCl_3$ was filtered (silica gel) to give **3** (19 mg; 97%), identified by IR and UV–VIS spectra.

Support of this research by DGICYT of MEC (Spain) through project PB92-0031 is acknowledged. The authors express their gratitude to the EPR services of the Centre d'Investigació i Desenvolupament (CSIC) and the Universitat de Barcelona.

References

1 For reviews see: J. S. Miller, A. J. Epstein and W. M. Reiff, *Chem. Rev.*, 1988, **88**, 201; *Acc. Chem. Res.*, 1988, **21**, 114; H. Iwamura, *Adv. Phys. Org. Chem.*, 1990, **26**, 179; D. A. Dougherty, *Acc. Chem. Res.*, 1991, **24**, 88; H. Iwamura and N. Koga, *Acc. Chem. Res.*, 1993, **26**, 346; H. Kurreck, *Angew. Chem., Int. Ed. Engl.*, 1993, **32**, 1409; J. S. Miller and A. J. Epstein, *Angew. Chem., Int. Ed. Engl.*, 1994, **33**, 385; A. Rajca, *Chem. Rev.*, 1994, **94**, 871.
2 D. Griller and K. U. Ingold, *Acc. Chem. Res.*, 1976, **9**, 13.
3 M. Ballester, *Acc. Chem. Res.*, 1985, **18**, 380 and references cited therein; M. Ballester, *Adv. Phys. Org. Chem.*, 1989, **25**, 267 and references cited therein.
4 J. Veciana, C. Rovira, O. Armet, V. M. Domingo, M. I. Crespo and

F. Palacio, *Mol. Cryst. Liq. Cryst*., 1989, **176**, 77; J. Veciana, C. Rovira, M. I. Crespo, O. Armet, V. M. Domingo and F. Palacio, *J. Am. Chem. Soc*., 1991, **113**, 2552; J. Carilla, L. Juliá, J. Riera, E. Brillas, J. A. Garrido, A. Labarta and R. Alcalá, *J. Am. Chem. Soc*., 1991, **113**, 8281; J. Veciana, C. Rovira, N. Ventosa, M. I. Crespo and F. Palacio, *J. Am. Chem. Soc*., 1993, **115**, 57; V. M. Domingo, J. Castañer, J. Riera and A. Labarta, *J. Org. Chem*., 1994, **59**, 2604; R. Chaler, J. Carilla, E. Brillas, A. Labarta, Ll. Fajarí, J. Riera and L. Juliá, *J. Org. Chem*., 1994, **59**, 4107; M. Ballester, I. Pascual, C. Carreras and J. Vidal-Gancedo, *J. Am. Chem. Soc*., 1994, **116**, 4205.

5 (*a*) J. Carilla, Ll. Fajarí, L. Juliá, J. Riera and Ll. Viadel, *Tetrahedron Lett*., 1994, **35**, 6529; (*b*) S. López, J. Carilla, Ll. Fajarí, L. Juliá, E. Brillas and A. Labarta, *Tetrahedron*, 1995, **51**, 7301; (*c*) J. Carilla, Ll. Fajarí, L. Juliá, J. Sañé and J. Rius, *Tetrahedron*, 1996, **52**, 7013.

6 L. Teruel, Ll. Viadel, J. Carilla, Ll. Fajarí, E. Brillas, J. Sañé, J. Rius and L. Juliá, *J. Org. Chem*., 1996, **61**, 6063.

7 (*a*) P. M. Lahti, A. S. Ichimura and J. A. Berson, *J. Org. Chem*., 1989, **54** 958; (*b*) *J. Org. Chem*., 1991, **56**, 3030; (*c*) C. Ling, M. Minato, P. M. Lahti and H. van Willigen, *J. Am. Chem. Soc*., 1992, **114**, 9959; (*d*) M. Minato, P. M. Lahti and H. van Willigen, *J. Am. Chem. Soc*., 1993, **115**, 4523; (*e*) N. Yoshioka, P. M. Lahti, T. Kaneko, Y. Kuzumaki, E. Tsuchida and H. Nishida, *J. Org. Chem*., 1994, **59**, 4272.

8 O. Armet, J. Veciana, C. Rovira, J. Riera, J. Castañer, E. Molins, J. Rius, C. Miravitlles, S. Olivella and J. Brichfeus, *J. Phys. Chem*., 1989, **91**, 5608.

9 Z. Galus, *Fundamentals of Electrochemical Analysis*, Harwood, Chichester, 1976, ch. 7, p. 9; H. Lund and M. M. Baizer, *Organic Electrochemistry. An Introduction and a Guide*, Marcel Dekker, New York, ch. 2, p. 3.

10 H. R. Falle, G. R. Lukhurst, A. Horsefield and M. Ballester, *J. Chem. Phys*., 1969, **50**, 258.

11 D. C. Reitz and S. I. Weissman, *J. Chem. Phys*., 1960, **33**, 700.

12 The distance between the two α-carbons has been calculated from standard angles and bond lengths, and assuming that the C—N bond length is 1.426 Å and the C—N—C angle is 108.0°.

13 A. M. Trozzolo, R. W. Murray and E. Wasserman, *J. Am. Chem. Soc*., 1962, **84**, 4990.

14 T. Mitsumori, K. Inoue, N. Koga and H. Iwamura, *J. Am. Chem. Soc*., 1995, **117**, 2467.

15 R. L. Carlin, *Magnetochemistry*, Springer-Verlag, Berlin, Heidelberg, 1986, p. 21.

Paper 7/07993A; *Received* 6*th November*, 1997